



Phenylene ethynylene azobenzenes with symmetrical peripheral chromophores: Synthesis, optical properties and photoisomerization behaviors study

Rui Liu, Qi Xiao, Yuhao Li, Hongbin Chen, Zhangwei Yan, Hongjun Zhu*

Department of Applied Chemistry, College of Science, Nanjing University of Technology, Nanjing 210009, PR China

ARTICLE INFO

Article history:

Received 21 March 2011

Received in revised form

5 June 2011

Accepted 7 June 2011

Available online 14 June 2011

Keywords:

Azobenzene

Phenylene ethynylene

Chromophores

Photoisomerization

Optical property

Synthesis

ABSTRACT

A series of phenylene ethynylene azobenzenes bearing different symmetrical peripheral chromophores were synthesized by Sonogashira coupling and characterized by UV–vis absorption, fluorescence emission, cyclic voltammetry and *cis*–*trans* photoisomerization. All compounds exhibit strong ${}^1\pi,\pi^*$ absorption bands in the UV region, which pronouncedly blue-shifts when the π -electron donating chromophore attached on the *para*-position of phenyl group. When excited at the ${}^1\pi,\pi^*$ band, the compounds exhibit violet to blue emission (363 ~ 430 nm), which is attributed to a ${}^1\pi,\pi^*$ emission. All of these compounds show reversible *trans*–*cis* isomerization in dichloromethane solution, indicating that the π -conjugated phenylene ethynylene backbone does not prevent the occurrence of the photochemical processes of the azobenzene center. The photoisomerization properties were influenced by the peripheral chromophores in the conjugated system and the steric interactions. In addition, the kinetic investigation of the photoisomerization process was carried out.

© 2011 Elsevier Ltd. All rights reserved.

1. Introduction

Photochromic compounds have attracted a great interest in recent years due to their intriguing spectroscopic properties and potential applications in photoresponsive materials, non-linear optics, micro-electronics and optical data storage [1–6]. Among these, azobenzene derivatives have been extensively investigated and gained enormous interest. As photoactive compounds, they can undergo reversible transformation from the thermodynamically stable *trans* form to the *cis* form by irradiation with UV or visible light. The back *cis*-to-*trans* reaction can be achieved by illumination with UV/vis light of a different wavelength or appears by thermal relaxation. This shift in structure causes a significant change in colour, refractive index, dielectric constant, dipole moment, etc., making azobenzenes potentially attractive in the realms of photoresponsive materials and non-linear optics [7–14].

Zeitouny and co-workers [8] have synthesized a series of ethynyl-bearing azobenzene compounds with suitably-designed peripheral groups. All of them exhibit reversible *trans*-to-*cis* isomerization in cyclohexane solution showing that π -delocalized appended fragments do not prevent the occurrence of the photochemical and thermal processes of the azoalkene center. Tour and co-workers [6,7,12] have also developed a class of novel oligo(phenylene ethynylene) azobenzene derivatives as potential molecular electronic

switching device candidates, which indicate that the oligo(phenylene ethynylene)s (OPEs) attached to an azobenzene moiety have a strong impact on its photoisomerization behavior. When they are combined together to form more complex systems, the present work underscores that their synergistic effects must be considered.

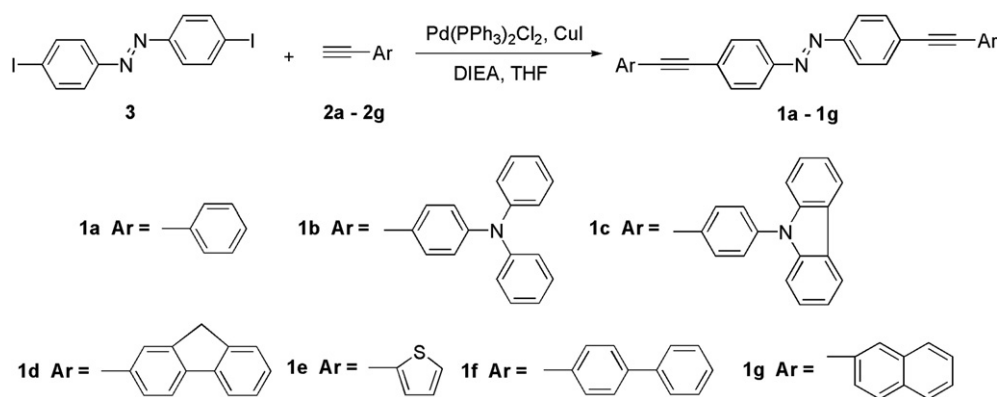
The reported work are quite intriguing, however, the study on azobenzene-OPE derivatives, especially the effect of various chromophores on their photophysics is still limited. In this context, the development of new phenylene ethynylene azobenzene derivatives coupled with various chromophores, also the further study of the photophysical properties, photoisomerization behaviors and structure–property relationships are feasible, challengeable, and valuable. To remedy this deficiency, our groups have designed and synthesized a series of new phenylene ethynylene azobenzenes derivatives with symmetrical peripheral chromophores (Scheme 1). Compound **1a** has been reported in the literature [7] and was synthesized as a reference. Their photophysical properties and photoisomerization behaviors have been investigated with the aim of understanding the structure–physical property relationships and developing potential photoresponsive materials.

2. Experimental

2.1. Materials

Bis(triphenylphosphine)palladium (II) dichloride was purchased from ABCR Chemical Ltd. Phenylacetylene (**2a**) and 4-ethynylbiphenyl

* Corresponding author. Tel.: +86 25 83172358; fax: +86 25 83587428.
E-mail address: zhuhjnjut@hotmail.com (H. Zhu).



Scheme 1. Synthesis of phenylene ethynylene azobenzene compounds (**1a** – **1g**).

(**2f**) were purchased from Sigma–Aldrich Company. Other reagents were purchased from Sinopharm Chemical Reagent Co. Ltd. and were used without any further purification. Tetrahydrofuran (THF) and *N,N*-diisopropylethylamine (DIEA) were distilled under N_2 over sodium benzophenone ketyl. Silica gel chromatography was carried out on silica gel (200–300 mesh). (*E*)-bis-(4-iodo-phenyl)-diazene (**3**) [15] and arylacetylide derivative **2b** [16,17], **2c** [18,19], **2e** [20,21], **2g** [22] were synthesized according to literature methods.

2.2. Measurements

Melting points were measured on an X-4 microscope electrothermal apparatus (Taikhe China) and were uncorrected. 1H NMR and ^{13}C NMR spectra were recorded on a Bruker AV-500 spectrometer at 500 MHz or a Bruker AV-300 spectrometer at 300 MHz using $CDCl_3$ or $DMSO-d_6$ as the solvent, with tetramethylsilane as internal standard. The elemental analyses were performed with a Vario El III elemental analyzer. Optical absorption spectra were obtained using an HP-8453 UV/vis/near-IR Spectrophotometer (Agilent). PL spectra were carried out on an LS-55 spectrofluorometer (Perkin–Elmer). High resolution mass (HRMS) analyses were performed at a Bruker BioToF III mass spectrometer (Bruker). The UV light for irradiation is generated by a 500 W mercury lamp cooled by a circulated cooling water system with two different light filters centered at 365 nm ($P = 0.35 W cm^{-2}$) and 254 nm ($P = 0.22 W cm^{-2}$) respectively. Azobenzene photoisomerization experiments were carried out using a 1 cm quartz cuvette to measure absorbance changes immediately after the sample solution in cuvette had been subject to UV light. The electrochemical experiments were carried out using a CHI 660C electrochemistry workstation (CHI USA). A standard one-compartment three-electrode cell was used with a Pt electrode as the working electrode, a Pt wire as the counter electrode and a Ag/Ag^+ electrode (Ag in 0.1 M $AgNO_3$ solution, from CHI, Inc.) as the reference electrode. TBAP (Tetrabutylammonium perchlorate, 0.1 M) was used as the supporting electrolyte and the scan rate was $100 mV s^{-1}$.

2.3. Synthesis

2.3.1. General procedure for synthesis of compound **1a–1g**

A mixture of compound **3** (0.43 g, 1 mmol, 1.0 equiv.), bis(triphenylphosphine) palladium (II) dichloride (0.035 g, 0.5 mol %), CuI (0.01 g, 0.5 mol%), DIEA (0.20 g, 1.6 mmol, 1.6 equiv.), arylacetylide derivative (1 mmol, 1.0 equiv.) in anhydrous THF (30 mL) was stirred for 24 h under a nitrogen atmosphere at 60 °C in the absence of light. The mixture was then quenched with water, extracted with CH_2Cl_2 ($3 \times 30 mL$), washed by brine, dried over

anhydrous $MgSO_4$ and evaporated to dryness. Then the crude product was purified by column chromatography (silica gel, hexane/ $CH_2Cl_2 = 6:1$, v/v) to give the desired product.

2.3.2. (*E*)-bis-(4-phenylethynyl-phenyl) diazene (**1a**)

Yield was 40.0% as orange solid; m.p. decomposes at 245 °C (Lit. [7]: 246 °C). 1H NMR ($CDCl_3$, 500 MHz): δ ppm 7.93 (d, $J = 8.6$ Hz, 4H), 7.68 (d, $J = 8.7$ Hz, 4H), 7.56–7.59 (m, 4H), 7.36–7.39 (m, 6H). ^{13}C NMR ($CDCl_3$, 300 MHz): δ ppm 152.2, 132.8, 132.3, 129.1, 128.9, 125.5, 123.5, 123.3, 92.8, 89.9. HRMS calcd for $C_{28}H_{18}N_2$: 382.1470. Found: 382.1465. Anal. calcd. (%) for $C_{28}H_{18}N_2$: C, 87.93; H, 4.74; N, 7.32. Found: C, 87.88; H, 4.78; N, 7.30.

2.3.3. (*E*)-bis-(4-(4-diphenylamino phenylethynyl) phenyl) diazene (**1b**)

Yield was 32% as orange solid; m.p. decomposes at 202 °C. 1H NMR ($DMSO-d_6$, 500 MHz): δ ppm 7.98 (d, $J = 8.5$ Hz, 4H), 7.67 (d, $J = 8.9$ Hz, 4H), 7.42 (d, $J = 8.5$ Hz, 4H), 7.27–7.34 (m, 8H), 7.09 (d, $J = 8.7$ Hz, 8H), 6.98–7.05 (m, 4H), 6.89 (d, $J = 8.7$ Hz, 4H). ^{13}C NMR ($DMSO-d_6$, 300 MHz): δ ppm 151.2, 151.0, 146.2, 138.5, 137.6, 132.7, 132.3, 129.9, 129.7, 126.4, 126.0, 125.2, 125.0, 124.4, 124.2, 123.0, 121.6, 120.8, 94.2, 89.2. HRMS calcd for $C_{52}H_{36}N_4$: 716.2940. Found: 716.2937. Anal. calcd. (%) for $C_{52}H_{36}N_4$: C, 87.12; H, 5.06; N, 7.82. Found: C, 87.08; H, 5.08; N, 7.84.

2.3.4. (*E*)-bis-(4-(4-carbazol-9-yl phenylethynyl) phenyl) diazene (**1c**)

Yield was 35% as orange solid; m.p. decomposes at 257 °C. 1H NMR ($CDCl_3$, 500 MHz): δ ppm 8.14 (d, $J = 7.0$ Hz, 4H), 7.95 (d, $J = 6.5$ Hz, 4H), 7.89 (d, $J = 7.0$ Hz, 4H), 7.72 (d, $J = 7.5$ Hz, 4H), 7.68 (d, $J = 7.5$ Hz, 4H), 7.61 (d, $J = 7.8$ Hz, 4H), 7.41–7.48 (m, 4H), 7.28–7.33 (m, 4H). ^{13}C NMR ($CDCl_3$, 300 MHz): δ ppm 151.9, 151.7, 140.5, 138.4, 138.1, 137.9, 133.2, 133.1, 132.5, 132.2, 126.8, 126.1, 124.5, 123.6, 123.1, 122.4, 121.8, 120.4, 120.3, 109.7, 101.8, 91.4, 90.0. HRMS calcd for $C_{52}H_{32}N_4$: 712.2627. Found: 712.2631. Anal. calcd. (%) for $C_{52}H_{32}N_4$: C, 87.62; H, 4.52; N, 7.86. Found: C, 87.88; H, 4.58; N, 7.84.

2.3.5. (*E*)-bis(4-(fluoren-2-yl ethynyl) phenyl) diazene (**1d**)

Yield was 38% as orange solid; m.p. decomposes at 260 °C. 1H NMR ($CDCl_3$, 500 MHz): δ ppm 7.92 (d, $J = 8.5$ Hz, 4H), 7.88 (d, $J = 8.5$ Hz, 2H), 7.81 (d, $J = 7.5$ Hz, 2H), 7.78 (d, $J = 8.0$ Hz, 2H), 7.75 (d, $J = 8.0$ Hz, 4H), 7.68 (d, $J = 7.5$ Hz, 2H), 7.58 (d, $J = 8.0$ Hz, 2H), 7.38–7.42 (m, 2H), 7.31–7.35 (m, 2H), 3.93 (s, 4H). ^{13}C NMR ($DMSO-d_6$, 300 MHz): δ ppm 152.1, 151.8, 143.6, 143.4, 131.4, 128.9, 127.7, 126.9, 125.2, 120.7, 120.4, 89.7, 86.8. HRMS calcd for $C_{42}H_{26}N_2$: 558.2096. Found: 558.2089. Anal. calcd. (%) for $C_{42}H_{26}N_2$: C, 90.29; H, 4.69; N, 5.01. Found: C, 90.18; H, 4.78; N, 5.14.

2.3.6. (*E*)-bis(4-(thiophen-2-yl ethynyl) phenyl) diazene (**1e**)

Yield was 36% as orange solid; m.p. decomposes at 230 °C. ¹H NMR (DMSO-*d*₆, 500 MHz): δ ppm 8.01 (d, *J* = 8.7 Hz, 4H), 7.79 (d, *J* = 8.5 Hz, 4H), 7.48–7.52 (m, 4H), 7.15–7.18 (m, 2H). ¹³C NMR (DMSO-*d*₆, 500 MHz): δ ppm 151.2, 151.1, 138.4, 135.9, 133.4, 133.3, 133.2, 132.6, 132.3, 131.8, 131.5, 129.6, 129.5, 128.0, 127.8, 125.0, 124.4, 123.2, 123.0, 122.8, 122.6, 121.3, 92.4, 91.8, 86.5, 85.5. HRMS calcd for C₂₄H₁₄N₂S₂: 394.0598. Found: 394.0588. Anal. calcd. (%) for C₂₄H₁₄N₂S₂: C, 73.07; H, 3.58; N, 7.10. Found: C, 73.08; H, 3.68; N, 7.04.

2.3.7. (*E*)-bis(4-(4-phenyl phenylethynyl) phenyl) diazene (**1f**)

Yield was 53% as yellow solid; m.p. decomposes at 199 °C. ¹H NMR (DMSO-*d*₆, 500 MHz): δ ppm 7.99 (d, *J* = 6.8 Hz, 4H), 7.76 (d, *J* = 7.0 Hz, 4H), 7.66–7.74 (m, 12H), 7.48–7.52 (m, 4H), 7.39–7.42 (m, 2H). ¹³C NMR (DMSO-*d*₆, 500 MHz): δ ppm 151.1, 141.4, 138.8, 138.4, 137.7, 132.9, 129.1, 128.0, 127.0, 126.6, 124.4, 124.1, 119.3, 95.3, 88.9, 82.8. HRMS calcd for C₄₀H₂₆N₂: 534.2096. Found: 534.2091. Anal. calcd. (%) for C₄₀H₂₆N₂: C, 89.86; H, 4.90; N, 5.24. Found: C, 89.88; H, 4.88; N, 5.23.

2.3.8. (*E*)-bis(4-(naphthalen-2-yl ethynyl) phenyl) diazene (**1g**)

Yield was 48% as yellow solid; m.p. decomposes at 173 °C. ¹H NMR (DMSO-*d*₆, 500 MHz): δ ppm 8.30 (s, 1H), 8.23 (s, 1H), 7.94–8.01 (m, 10H), 7.65–7.68 (m, 4H), 7.63–7.64 (m, 2H), 7.58–7.62 (m, 4H). ¹³C NMR (DMSO-*d*₆, 500 MHz): δ ppm 151.0, 138.4, 133.0, 132.9, 132.5, 132.4, 132.3, 131.1, 128.5, 128.3, 128.0, 127.9, 127.8, 127.7, 127.6, 127.1, 127.0, 126.8, 124.3, 119.5, 117.6, 95.3, 90.0, 83.8, 82.9. HRMS calcd for C₃₆H₂₂N₂: 482.1783. Found: 482.1779. Anal. calcd. (%) for C₃₆H₂₂N₂: C, 89.60; H, 4.60; N, 5.81. Found: C, 89.88; H, 4.68; N, 5.84.

3. Results and discussions

3.1. Synthesis and characterization

Scheme 1 outlines the synthesis of the phenylene ethynylene azobenzene derivatives with symmetrical peripheral chromophores. The Pd/Cu-catalyzed Sonogashira coupling reactions yielded the desired final products in 32–53% yields. All the products are air-stable and soluble in CH₂Cl₂, CHCl₃, tetrahydrofuran, dimethylformamide (DMF) and dimethyl sulphoxide (DMSO) in varying degrees. ¹H NMR spectra, ¹³C NMR spectra, HRMS and element analysis on **1a–1g** confirmed the proposed structures. The NMR data for all of the compounds are consistent with the assigned structures and previously reported compound of this type [7,8,12].

3.2. UV–vis absorption

The UV–vis absorption spectra of **1a–1g** in CH₂Cl₂ solution at room temperature are presented in Fig. 1, the band of absorption maxima and molar extinction coefficients for each compound are compiled in Table 1. The absorption obeys Lambert–Beer's law in the concentration range studied ($1 \times 10^{-6} \sim 1 \times 10^{-4}$ mol/L), suggesting no dimerization or oligomerization occurs within this concentration range. As shown in Fig. 1, all the compounds exhibit intense absorption bands between 330 and 390 nm, which are assigned to $\pi-\pi^*$ electronic transitions. Meanwhile, the characteristic azobenzene bands, namely the $n-\pi^*$ electronic transition bands between 400 and 500 nm, are no longer distinguishable and overlapped by the $\pi-\pi^*$ bands. In accord with the previous work on azobenzene systems [3,8,10,13], the azobenzene central unit is involved in extended π -conjugation all the way to the terminal units, which are known to promote low-lying charge transfer absorption bands. In the case of **1b**, an additional broad moderate band at 425 nm was observed, which can be attributed to the intramolecular

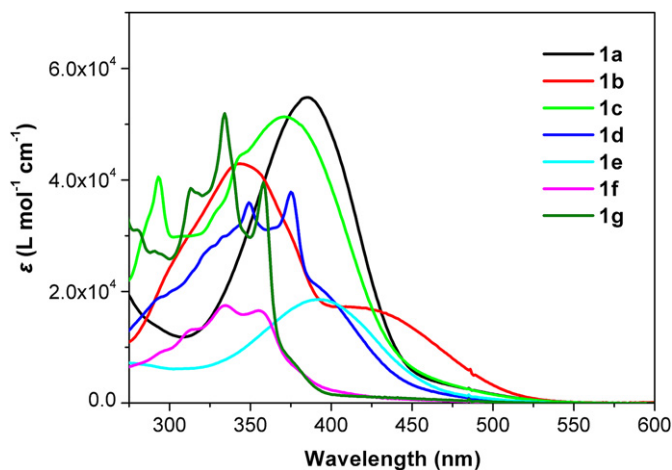


Fig. 1. UV–Vis absorption spectra of **1a–1g** in CH₂Cl₂ solution (10^{-5} mol/L).

charge transfer (ICT) transitions originated from the diphenylamine moiety. Compared with the ground state absorption of the core structure compound 4,4'-diethynylazobenzene [8], these derivatives (**1a–1g**) exhibit a dramatic increase of absorption intensity and a marked shift to lower energy of the intense $\pi-\pi^*$ transition band.

Compared with **1a** and **1e** (Fig. 1), **1c**, **1d**, **1f** and **1g** exhibit more structured absorption bands in the range of 300–375 nm, which may arise from the $\pi-\pi^*$ transitions feature of the π -conjugated chromophores. The $\pi-\pi^*$ transitions appearing are influenced significantly by the nature of the peripheral chromophores. Compared with **1a**, the electron donating substituents appended on the *para*-position of phenyl group, such as NPh₂ and carbazolyl, cause a pronounced blue-shift of this transition. The π -electron donating substituents such as fluorenyl, biphenyl and naphthyl, instead of the phenyl group, also induced a significant blue-shift compared to **1a**. However, it is noted that in the case of **1e**, the π -electron donating heterocycle substituent thienyl causes a red-shift of 8 nm compared to **1a**. Considering the π -electron delocalization and the presence in *cis*-isomers of strained conformations, the electron donating ability of the substituent and the existence of *cis*-isomers should both influence the ground state absorption properties of these azo compounds. Optical band gaps (E_g^{Opt}) determined from the absorption edge of the solution spectra are given in Table 1, which varies from 2.41 eV in **1b** to 3.11 eV in **1g**.

3.3. Emission

The emission characteristics of compounds **1a–1g** in CH₂Cl₂ at room temperature were investigated, and their normalized emission spectra at a concentration of 1×10^{-7} mol/L are illustrated in

Table 1
Photophysical properties of **1a–1g** recorded in CH₂Cl₂ solution.^a

Compound	$\lambda^{\text{Abs}}_{\text{max}}/\text{nm}$	$\epsilon/10^3$ L mol ⁻¹ cm ⁻¹	$\lambda^{\text{Em}}_{\text{max}}/\text{nm}$	Stokes shift (nm)	$\Phi_{\text{em}}^{\text{b}}$	E_g^{Opt} (eV)
1a	385	54.8	426	41	0.02	2.79
1b	344	42.9	378	34	0.06	2.41
1c	371	51.2	404	33	0.15	2.76
1d	375	37.8	401	26	0.13	2.76
1e	393	18.6	430	37	0.27	2.65
1f	334	17.5	371	37	0.19	3.05
1g	333	51.6	363	30	0.06	3.11

^a Measured in degassed CH₂Cl₂ solutions at 298 K.

^b 9,10-Diphenylanthracene as reference ($\Phi_{\text{F}} = 0.90$ in cyclohexane).

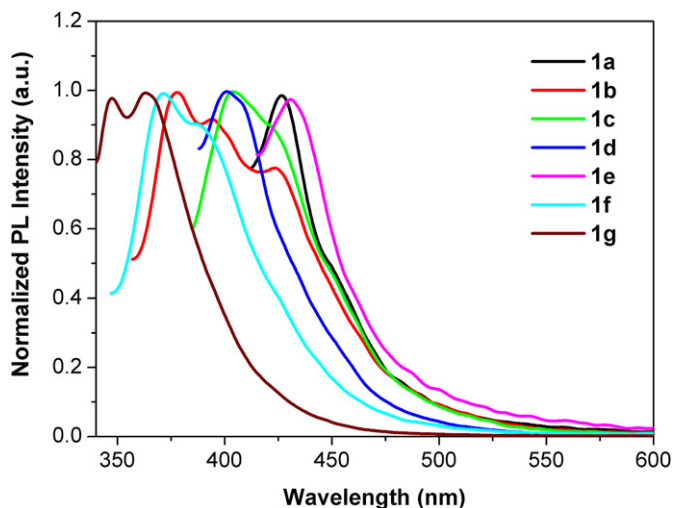


Fig. 2. Emission spectra of **1a–1g** in CH_2Cl_2 solution (10^{-7} mol/L).

Fig. 2. As shown in Fig. 2 and Table 1, excitation of these compounds at their respective absorption band maximum results in weak violet to blue luminescence, corresponding to a Stokes shift of 26 ~ 41 nm. The relatively small Stokes shift and structured emission spectra suggest that observed emission from these compounds are originated from $\pi-\pi^*$ singlet excited state. In contrast, the emission energies (λ_{max} , nm) of **1a–1g** are influenced by the nature of the ancillary substituents. Compared with **1a**, the appended electron donating substituents NPh_2 and carbazolyl, cause a blue-shift of the emission maxima. Meanwhile, when the π -electron donating substituents attached instead of the phenyl group, such as fluorenyl in **1c**, biphenyl in **1f** and naphthyl in **1g**, these compounds also show a pronounced blue-shift of the emission band compared to **1a**. Except for **1e**, the band of absorption maxima of all the other compounds exhibit an obvious blue-shift compared to **1a**, which increase in the order of **1e** > **1a** > **1c** > **1d** > **1b** > **1f** > **1g**. This trend is consistent with that observed for the absorption bands in the UV–vis absorption spectra. This suggests that the emitting state for **1a–1g** could be possibly be dominated by the electron donating ability of the substituent and the existence of strained conformations from *cis*-isomers. Additionally, the emission quantum yields of these compounds are relatively low in the range of 0.02~0.27

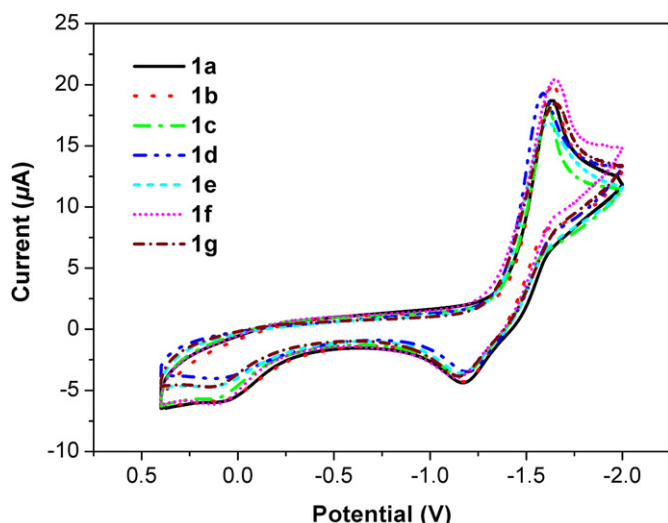


Fig. 3. Cyclic voltammetry of **1a–1g** in DMF solution.

Table 2
Electrochemistry data of compound **1a–1g**.^a

Compound	$E_{\text{ox}}^{\text{peak}}$ (V)	$E_{\text{ox}}^{\text{onset}}$ (V)	$E_{\text{red}}^{\text{peak}}$ (V)	$E_{\text{red}}^{\text{onset}}$ (V)	LUMO ^b (eV)	HOMO ^b (eV)
1a	0.03	-0.31	-1.63	-1.35	3.05	5.84
1b	0.04	-0.29	-1.64	-1.41	2.99	5.40
1c	0.09	-0.24	-1.61	-1.35	3.05	5.81
1d	0.04	-0.40	-1.59	-1.37	3.03	5.79
1e	0.08	-0.21	-1.61	-1.35	3.05	5.70
1f	0.09	-0.20	-1.65	-1.39	3.01	6.06
1g	0.11	-0.19	-1.65	-1.33	3.07	6.18

^a All potentials vs SCE reference.

^b EA (LUMO) = $E_{\text{red}}^{\text{onset}} + 4.4$ eV; the HOMO energies are estimated according to the optical band gap and the LUMO energy values from electrochemical experimental results.

using 9,10-diphenylanthracene (0.90 in cyclohexane) as reference, which were found in the order of **1e** > **1f** > **1c** > **1d** > **1g** > **1b** > **1a**. When the conjugation length of the phenylacetylide chromophores extends, the corresponding emission quantum yield increases. Notably, compound **1e** exhibits the highest emission quantum yield in this series, we tentatively propose that the quantum yields were influenced by their *trans-cis* inter-conversions.

It is well known that the azobenzene moiety does not show any fluorescence because azobenzene is characterized by a shallow minima for singlet and triplet levels of both $\pi-\pi^*$ and $n-\pi^*$ electronic configuration. As a consequence, the non-irradiative processes, which include *trans-cis* inter-conversion, are very fast and compete efficiently with radiative process [8,9]. The azobenzene unit has a strong impact on the photoluminescence of all the compounds. By considering the weak emission and low quantum yields of these compounds, we propose that the emission of the substituted peripheral chromophores is partly reabsorbed by the strong azobenzene absorption band, and the fluorescent excited state of the chromophoric moiety is quenched by the azobenzene unit, which is in line with the properties of azobenzenes reported in literatures [3,4,6,8–10].

3.4. Electrochemical properties

The electrochemical behaviors of **1a–1g** were investigated by cyclic voltammetry (CV) in dry DMF solutions at 298 K (Fig. 3). In general, the cyclic voltammograms exhibit one reversible reduction couple with $E_{1/2}$ in the range of -1.59 to -1.65 V versus $\text{Cp}_2\text{Fe}^{+/0}$,

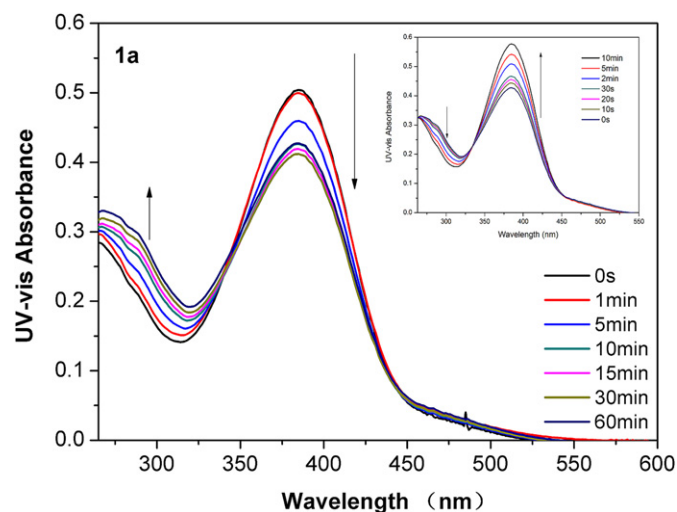


Fig. 4. Time evolution of the absorption spectra of *trans*-**1a** in CH_2Cl_2 solution (10^{-5} mol/L) under 365 nm light irradiation, until PSS is reached in 60 min. Inset: Back reaction observed over time under 254 nm light irradiation.

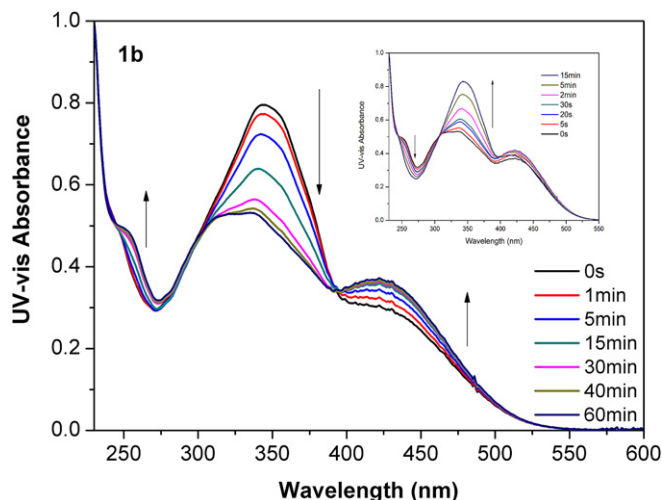


Fig. 5. Time evolution of the absorption spectra of *trans*-**1b** in CH_2Cl_2 solution (10^{-5} mol/L) under 365 nm light irradiation, until PSS is reached in 60 min. Inset: Back reaction observed over time under 254 nm light irradiation.

which originates from the reduction of the azobenzene moiety [7], and does not show obvious dependence on different peripheral chromophores. During the process of anodic scan, all compounds were observed an irreversible oxidation wave at 0.03–0.11 V, which can be assigned to the π -electron conjugated chromophore segments. The electro-donating groups on the *para*-position of the phenyl group shift the oxidation waves to more positive direction. For example, the electron-donating group NPh_2 and carbazolyl shift the oxidation wave to 0.04 and 0.09 V, while this oxidation occurs at 0.03 for compound **1a** which has no substituent on its phenyl unit. The conjugation length of the phenyl acetylene chromophore segments also influence the oxidation. The π -electron donating substituents such as fluorenyl, biphenyl, naphthyl and thienyl, instead of the phenyl group, shift the oxidation waves to more positive direction significantly. Electron affinities (lowest unoccupied molecular orbital, LUMO) were estimated from the onset of the reduction wave ($EA = E_{\text{red}}^{\text{onset}} + 4.4$) by using an SCE energy level of 4.4 eV versus a vacuum [23–27]. All eight compounds have electron affinities between 2.99 and 3.07 eV (below vacuum), revealing low energy barriers to electron injection from the cathode. Compared to **1a**, the appended electron donating substituents NPh_2 and carbazolyl make the band gaps decreased. Meanwhile, when the π -electron donating substituents attached on the acetylene unit instead of the phenyl group, such as fluorenyl in **1c** and thienyl in **1e**, the band gaps also show a pronounced decrease compared to **1a**. For biphenyl in **1f** and naphthyl in **1g**, the band gaps between HOMO and LUMO increase compared to **1a**, which are tentatively assigned to the influence of the existence of *cis*-isomers to their electron structure properties. Detailed data for the CV and energy level parameters are listed in Table 2.

Table 3
Photoisomerization data of compound **1a–1g**.^a

Compound	Abs _{max} at PSS under 365 nm	C ₃₆₅ (<i>trans</i> -isomer)/%	Abs _{max} at PSS under 254 nm	C ₂₅₄ (<i>trans</i> -isomer)/%	$k_1/10^{-6} \text{ s}^{-1}$	$k_2/10^{-6} \text{ s}^{-1}$
1a	0.42	81.6	0.58	93.7	281.3	3021.6
1b	0.53	65.7	0.82	91.0	383.3	1160.0
1c	0.45	87.1	0.59	94.9	233.7	8423.7
1d	0.35	90.0	0.40	98.1	131.2	4727.5
1e	0.41	92.4	0.49	98.2	91.2	10023.3
1f	0.36	76.3	0.46	97.8	332.8	1135.3
1g	0.53	86.5	0.58	97.4	285.8	1575.6

^a Apparent first-order rate constant k_1 for *trans*–*cis* photoisomerization under 365 nm irradiation, first-order rate constant k_2 for *cis*–*trans* photoisomerization under 254 nm irradiation, the *trans*-isomer content at the PSS under 365 nm irradiation (C₃₆₅), and the *trans*-isomer content at the PSS under 254 nm irradiation (C₂₅₄).

3.5. Photoisomerization studies

The Phenylene ethynylene azobenzenes **1a–1g** were subjected to photoisomerization experiments and monitored using UV–vis spectroscopy with the aim of probing the occurrence of *cis*–*trans* or *trans*–*cis* isomerization in dichloromethane solution. Before the optical measurement, the sample solutions were kept in dark for several days at room temperature and at elevated temperature, about 60 °C, for several hours, to ensure that all of the azobenzene units were in *trans* form. This process could be monitored by observing the absorption peak increasing of *trans* form π – π^* transition until the absorbance reached a maximum value. Preliminary tests showed that after more than ten cycles of UV light induced *trans*–*cis* and *cis*–*trans* isomerization cycles, the peak values and positions were still maintained without noticeable change. The initial *trans* spectrum is fully recovered showing complete reversibility.

Irradiation of **1a** solution at 365 nm with UV light results in photoisomerization from the *trans*- to the *cis*-isomer, as evidenced in Fig. 4, by a decrease in absorbance at about 385 nm and an increase at about 290 nm. The isosbestic points at 346 and 443 nm indicated that the azobenzene isomerization was the only process and was a reversible photoreaction. A photostationary state (PSS) is reached within 60 min of irradiation, whereas by changing the irradiation wavelength (254 nm), the spectral profile of the starting *trans*-samples is fully recovered in just 10 min. Full reversibility of this *cis* to *trans* process can also be observed by keeping the solution in the dark for two hours, and similar photoisomerizations are observed for a large number of azobenzenes [4,8–10,13]. Compared to the absorption spectra of 4,4'-diethynylazobenzene reported by Zeitouny group [8], the characteristic azobenzene bands are not obvious in **1a** because the azobenzene central unit is involved in extended OPEs π -conjugated system, which could promote low-lying and intense charge transfer absorption bands.

The photoisomerization spectrum of **1b**, as another example, is illustrated in Fig. 5. The process exhibits similar trend as **1a** and prompts reversibility, showing that the forward and back isomerization processes also occurred in **1b**. However, it is noted that the irradiation of **1b** with UV light results in the increase of the ICT absorbance at 425 nm, and a strong decrease of the π – π^* absorbance accompanied by a blue-shift of the maximum from 344 nm to 335 nm, due to the formation of the *cis* isomer. The sharp isosbestic points can also be observed clearly, indicating that the only process and reversible photoreaction. When the photoisomerization experiments carried out with other phenylene ethynylene azobenzenes (**1c–1g**), the effects of the irradiation are nearly the same and only some fine distinctions can be observed (Fig. S1–S5). The all observed reversibility of the photochemical process goes along with: (1) the observation of clean isosbestic points; (2) the shorter irradiation times needed to accomplish the back photoreaction; (3) the occurrence of thermal back-reaction [10].

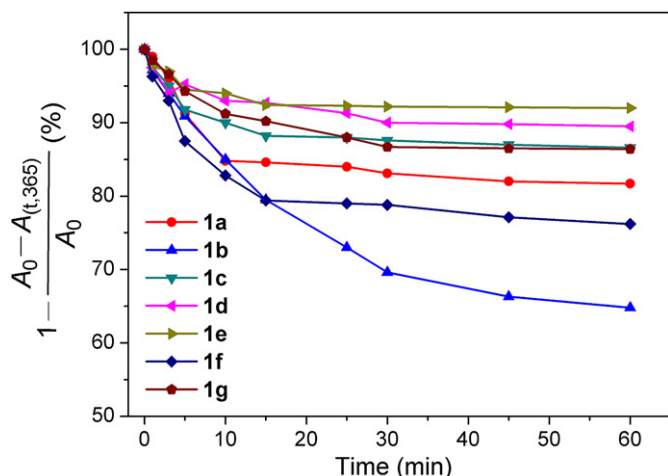


Fig. 6. Changes in the *trans*-fractions as a function of irradiation time for *trans*-to-*cis* photoisomerization in CH_2Cl_2 solution (10^{-5} mol/L).

Under the experimental conditions used, the content of *cis*-isomer at the PSS was calculated by $(A_0 - A_{(t,365)})/A_0$, where A_0 and $A_{(t,365)}$ are the absorption maxima of the unirradiated solution and of the solution at time t under 365 nm irradiation, respectively [4,28]. The corresponding content of *trans*-isomer at the PSS under 365 nm irradiation (C_{365}) for **1a–1g** are listed in Table 3, and the changes in the *trans*-fractions as a function of irradiation time for *trans*-to-*cis* photoisomerization are plotted in Fig. 6. As can be seen in Fig. 6 and Table 3, the content of *trans*-isomer decreases with the time evolution under 365 nm irradiation. The result clearly indicates that with different peripheral chromophores attached on the azobenzene, the photoisomerization yield at the PSS varies in different grade. The photoresponsive behavior of the azobenzene appended with peripheral chromophores is dependent on their structures, which is consistent with previous work on azobenzene reported by Mullen group [4]. Notably, the content of *trans*-isomer for **1b** decreased to 65.7% at the PSS, whereas the content of *trans*-isomer for **1e** just reached to 92.4% at the PSS. The electron donating ability of the substituent and the existence of *cis*-isomers could both influence the photoresponsive behaviors of these azo compounds, which may arise from the electron delocalization in the π -conjugated system as well as the presence of strained conformations.

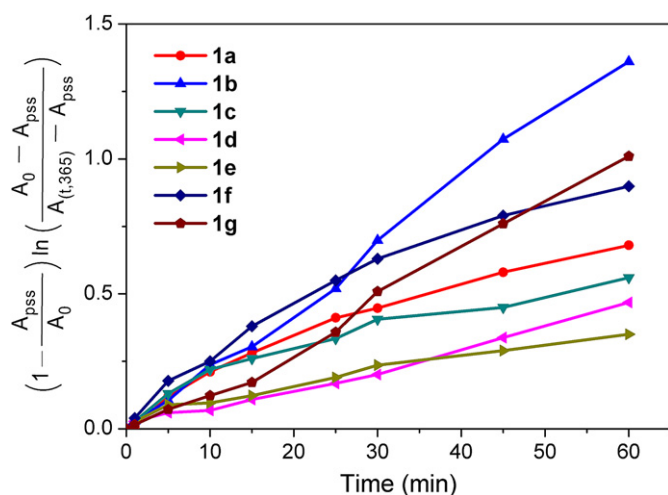


Fig. 7. The first kinetic reaction relation of the *trans*-to-*cis* photoisomerization in CH_2Cl_2 under 365 nm light irradiation.

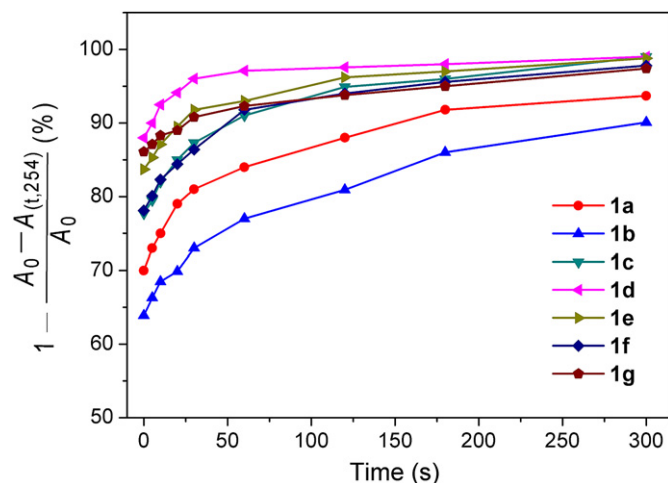


Fig. 8. Changes in the *trans*-fractions as a function of time for *cis*-to-*trans* isomerization in CH_2Cl_2 solution (10^{-5} mol/L).

The apparent first-order rate constant k_1 for *trans*-*cis* photoisomerization under 365 nm irradiation is determined from a plot of $(1 - A_{\text{PSS}(365)}/A_0) \ln[(A_0 - A_{\text{PSS}(365)})/(A_{(t,365)} - A_{\text{PSS}(365)})] \sim t$, where $A_{(t,365)}$ is the absorption maximum at time t under 365 nm irradiation (Fig. 7 and Table 3). It is evident from the comparison of the first order plots shown in Fig. 7 that the photoisomerization rate is affected by the phenylene ethynylene moieties, which follows the trend of **1b** > **1f** > **1g** > **1a** > **1c** > **1d** > **1e**. We would presume that the observed decrease in the photoisomerization yield and slow photoisomerization rate can be attributed to the constrained molecular motion of azobenzene in the conjugated system and the steric interactions caused by the increased conjugation effect. This interpretation is based on the findings and the interpretation of the similar behavior of OPE-azobenzene derivatives reported by Tour group [6].

While using 254 nm light for irradiation from the PSS obtained, the content of the *trans*-isomer is greatly enhanced. The content of *cis*-isomer at the PSS under 254 nm irradiation (C_{254}) for **1a–1g** were also calculated by $(A_0 - A_{(t,254)})/A_0$, where A_0 and $A_{(t,254)}$ are the absorption maxima of the unirradiated solution and of the solution at time t upon irradiation at 254 nm. The changes in the *trans*-fractions as a function of irradiation time for *cis*-to-*trans* photoisomerization are illustrated in Fig. 8. The apparent first-order rate constant k_2 for *cis*-to-*trans* isomerizations were determined by a plot of $\ln[(A_0 - A_{\text{PSS}(254)})/(A_0 - A_{(t,254)})] \sim t$ (Fig. 9), which are also listed in Table 3.

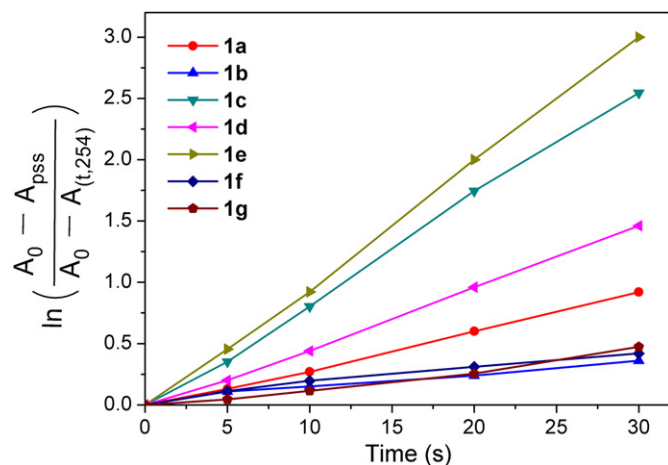


Fig. 9. The first kinetic reaction relation of the *cis*-to-*trans* isomerization in CH_2Cl_2 under 254 nm light irradiation.

As seen in Fig. 8, the content of *trans*-isomer for **1a**–**1g** increased obviously with the time evolution under 254 nm irradiation, which is analogous to the *trans*–*cis* isomerization and follows the trend of **1b** > **1a** > **1c** > **1g** > **1f** > **1d** > **1e**. It is important to note that the reaction rate of the *cis*–*trans* isomerization is much faster than that of the *trans*–*cis* photoisomerization induced by UV irradiation. As seen the first-order rate constant k_2 for *cis*–*trans* isomerization in Table 3, the thienyl (**1e**) and carbazolyl (**1c**) substituted derivative have notable recovery data compared to the other compounds. These rather anomalous fast recovery rates can be attributed to *cis*-isomers trapped in a strained conformation, and the peripheral chromophores incorporated with phenylene ethynylene lead to some photoinduced electron-transfer reactions. It seems that the photoisomerization of the azobenzene derivatives is more or less dependent on their structures which need more thorough study in their electrochemical properties and electronic structures. Furthermore, The steric effect has only a slight influence on the rate of the *trans*–*cis* photoisomerization and the reverse photoreaction which is in accord with the work by Schryver and co-workers [4].

4. Conclusions

In summary, a series of phenylene ethynylene azobenzenes with symmetrical peripheral chromophores were synthesized and characterized by UV–vis absorption, fluorescence emission, cyclic voltammetry and photoisomerization studies. The UV absorption and emission maxima of these compounds are influenced significantly by the nature of the peripheral chromophores. The π -electron donating chromophore causes a pronounced blue-shift in both UV absorption and emission spectra. The fluorescent excited state of the phenylene ethynylene chromophoric moiety is partly quenched by the azobenzene unit. Furthermore, the electrochemical properties, the *cis*–*trans* photoisomerization behaviors and first-order rate constants for the photoisomerization were investigated. The π -conjugated phenylene ethynylene backbone does not prevent the occurrence of the photochemical processes of the azobenzene center. The photoisomerization properties were influenced by the peripheral chromophores in the conjugated system and the steric interactions caused by the increased conjugation effect. We hope these compounds would contribute to the application of photo-responsive materials, and also serve as a model system for investigating structure–property relationships with respect to the nonlinear optical properties of phenylene ethynylene azobenzenes.

Acknowledgment

The authors acknowledge the National High Technology Research and Development Program (“863” Program) of China (2009AA032901), the Postgraduate Innovation Fund of Jiangsu Province (2009, CX09B_141Z) and the Doctor Thesis Innovation Fund of Nanjing University of Technology (2008, BSCX200812) for financial support.

Appendix. Supplementary information

Supplementary data associated with this article can be found in the online version, at doi:10.1016/j.dyepig.2011.06.006.

References

- [1] Ning Z, Tian H. Triarylamine: a promising core unit for efficient photovoltaic materials. *Chem Commun* 2009;37:5483–95.

- [2] Okano K, Tsutsumi O, Shishido A, Ikeda T. Azotolane liquid-crystalline polymers: huge change in birefringence by photoinduced alignment change. *J Am Chem Soc* 2006;128(48):15368–9.
- [3] Liao LX, Stellacci F, McGrath DV. Photoswitchable flexible and shape-persistent dendrimers: comparison of the interplay between a photochromic azobenzene core and dendrimer structure. *J Am Chem Soc* 2004;126(7):2181–5.
- [4] Grebel-Koehler D, Liu D, De Feyter S, Enkelmann V, Weil T, Engels C, et al. Synthesis and photomodulation of rigid polyphenylene dendrimers with an azobenzene core. *Macromolecules* 2003;36(3):578–90.
- [5] Raposo MMM, Fonseca AMC, Castro MCR, Belsley M, Cardoso MFS, Carvalho LM, et al. Synthesis and characterization of novel diazenes bearing pyrrole, thio-phenylene and thiazole heterocycles as efficient photochromic and nonlinear optical (NLO) materials. *Dyes Pigments* 2011;91(1):62–73.
- [6] Shirai Y, Sasaki T, Guerrero JM, Yu B-C, Hodge P, Tour JM. Synthesis and photoisomerization of fullerene - and oligo(phenylene ethynylene)-azobenzene derivatives. *ACS Nano* 2007;2(1):97–106.
- [7] Flatt AK, Dirk SM, Henderson JC, Shen DE, Su J, Reed MA, et al. Synthesis and testing of new end-functionalized oligomers for molecular electronics. *Tetrahedron* 2003;59(43):8555–70.
- [8] Zeitouny J, Aurisicchio C, Bonifazi D, Zorzi RD, Geremia S, Bonini M, et al. Photoinduced structural modifications in multicomponent architectures containing azobenzene moieties as photoswitchable cores. *J Mater Chem* 2009;19:4715–24.
- [9] Xia X, Gan LH, Hu X. The synthesis and properties of novel, functional azobenzene based metal complexes. *Dyes Pigments* 2009;83(3):291–6.
- [10] Freyer W, Brete D, Schmidt R, Gahl C, Carley R, Weinelt M. Switching behavior and optical absorbance of azobenzene-functionalized alkanethiols in different environments. *J Photochem Photobiol A* 2009;204(2–3):102–9.
- [11] Son H-J, Han W-S, Lee KH, Jung HJ, Lee C, Ko J, et al. Electrochemical deposition of end-capped triarylamine and carbazole dendrimers: alternate technique for the manufacture of multilayer films. *Chem Mater* 2006;18(25):5811–3.
- [12] Yu B-C, Shirai Y, Tour JM. Syntheses of new functionalized azobenzenes for potential molecular electronic devices. *Tetrahedron* 2006;62(44):10303–10.
- [13] Zarwell S, Ruck-Braun K. Synthesis of an azobenzene-linker-conjugate with tetrahedral shape. *Tetrahedron Lett* 2008;49(25):4020–5.
- [14] Chen Z, Dong S, Zhong C, Zhang Z, Niu L, Li Z, et al. Photoswitching of the third-order nonlinear optical properties of azobenzene-containing phthalocyanines based on reversible host-guest interactions. *J Photochem Photobiol A* 2009;206:213–9.
- [15] Barman DC, Saikia P, Prajapati D, Sandhu JS. Heterogeneous permanganate oxidations. A novel method for deamination reactions using solid supported iron-permanganate. *Synth Commun* 2002;32(22):3407–12.
- [16] Xiao H, Shen H, Lin Y, Su J, Tian H. Spirosilabifluorene linked bistrisphenylamine: synthesis and application in hole transporting and two-photon fluorescent imaging. *Dyes Pigments* 2006;73(2):224–9.
- [17] Maya F, Chanteau SH, Cheng L, Stewart MP, Tour JM. Synthesis of fluorinated oligomers toward physical vapor deposition molecular electronics candidates. *Chem Mater* 2005;17(6):1331–45.
- [18] Adhikari RM, Mondal R, Shah BK, Neckers DC. Synthesis and photophysical properties of carbazole-based blue light-emitting dendrimers. *J Org Chem* 2007;72(13):4727–32.
- [19] Flatt AK, Yao Y, Maya F, Tour JM. Orthogonally functionalized oligomers for controlled self-assembly. *J Org Chem* 2004;69(5):1752–5.
- [20] Liu R, Chang J, Xiao Q, Li Y, Chen H, Zhu H. The synthesis, crystal structure and photophysical properties of mononuclear platinum(II) 6-phenyl-[2,2']bipyridinyl acetylide complexes. *Dyes Pigments* 2011;88(1):88–94.
- [21] Fujimoto K, Shimizu H, Furusyo M, Akiyama S, Ishida M, Furukawa U, et al. Photophysical properties of 1,3,6,8-tetrakis(arylethynyl)pyrenes with donor or acceptor substituents: their fluorescence solvatochromism and light fastness. *Tetrahedron* 2009;65(45):9357–61.
- [22] Hwang J-J, Tour JM. Combinatorial synthesis of oligo(phenylene ethynylene)s. *Tetrahedron* 2002;58(52):10387–405.
- [23] Liu S, Wang Q, Jiang P, Liu R, Song G, Zhu H, et al. The photo- and electrochemical properties and electronic structures of conjugated diphenylanthrazolines. *Dyes Pigments* 2010;85:51–6.
- [24] Promarak V, Pankvung A, Ruchirawat S. Synthesis and characterization of novel *N*-carbazole end-capped oligothiophene-fluorenes. *Tetrahedron Lett* 2007;48(7):1151–4.
- [25] Promarak V, Saengsuwan S, Jungsuttiwong S. Synthesis and characterization of *N*-carbazole end-capped oligofluorenes. *Tetrahedron Lett* 2007;48(1):89–93.
- [26] Promarak V, Ichikawa M, Sudyoosuk T. Synthesis of electrochemically and thermally stable amorphous hole-transporting carbazole dendronized fluorene. *Synth Met* 2007;157(1):17–22.
- [27] Promarak V, Pankvung A, Jungsuttiwong S. Synthesis, optical, electrochemical, and thermal properties of α,α' -bis(9,9-bis-*n*-hexylfluorenyl)-substituted oligothiophenes. *Tetrahedron Lett* 2007;48(21):3661–5.
- [28] Morishima Y, Tsuji M, Kamachi M, Hatada K. Photochromic isomerization of azobenzene moieties compartmentalized in hydrophobic microdomains in a microphase structure of amphiphilic polyelectrolytes. *Macromolecules* 1992;25(17):4406–10.